X-ray structure of a protein-conducting channel

Bert van den Berg[1]*, William M. Clemons Jr[1]*, Ian Collinson[2], Yorgo Modis[3], Enno Hartmann[4], Stephen C. Harrison[3] & Tom A. Rapoport[1]

[1]*Howard Hughes Medical Institute and Department of Cell Biology, Harvard Medical School, 240 Longwood Avenue, Boston, Massachusetts 02115, USA*
[2]*Max Planck Institute of Biophysics, Marie-Curie-Strasse 13-15, D-60439 Frankfurt am Main, Germany*
[3]*Howard Hughes Medical Institute, Children's Hospital and Harvard Medical School, 320 Longwood Avenue, Boston, Massachusetts 02115, USA*
[4]*University Luebeck, Institute for Biology, Ratzeburger Allee 160, Luebeck, D-23538, Germany*

* These authors contributed equally to this work

A conserved heterotrimeric membrane protein complex, the Sec61 or SecY complex, forms a protein-conducting channel, allowing polypeptides to be transferred across or integrated into membranes. We report the crystal structure of the complex from *Methanococcus jannaschii* at a resolution of 3.2 Å. The structure suggests that one copy of the heterotrimer serves as a functional translocation channel. The α-subunit has two linked halves, transmembrane segments 1–5 and 6–10, clamped together by the γ-subunit. A cytoplasmic funnel leading into the channel is plugged by a short helix. Plug displacement can open the channel into an 'hourglass' with a ring of hydrophobic residues at its constriction. This ring may form a seal around the translocating polypeptide, hindering the permeation of other molecules. The structure also suggests mechanisms for signal-sequence recognition and for the lateral exit of transmembrane segments of nascent membrane proteins into lipid, and indicates binding sites for partners that provide the driving force for translocation.

A decisive step in the biosynthesis of many secretory and plasma-membrane proteins is their transport across the endoplasmic reticulum (ER) membrane in eukaryotes or across the cytoplasmic membrane in prokaryotes (for a review, see ref. 1). These polypeptides are first targeted to the membrane by hydrophobic amino-acid sequences, which are either cleavable signal sequences or transmembrane segments (TM) of membrane proteins. Soluble proteins, such as those destined for secretion, are subsequently transported across the membrane through a protein-conducting channel with a hydrophilic interior[2,3]. In the case of membrane proteins, when a hydrophobic TM arrives in the channel, it is released through an opening in the channel wall into the surrounding lipid phase. The capacity of the channel to open laterally towards the lipid and the wide variety of substrates that it must transport distinguish it from many other channels.

An evolutionarily conserved heterotrimeric complex of membrane proteins, called the Sec61 complex in eukaryotes and the SecY complex in eubacteria and archaea, forms the channel (for a review, see ref. 4). The α-subunits (Sec61α in mammals, Sec61p in *Saccharomyces cerevisiae*, SecY in bacteria and archaea) and γ-subunits (Sec61γ in mammals, Sss1p in *S. cerevisiae*, SecE in bacteria and archaea) show significant sequence conservation (see Supplementary Fig. S1). Both subunits are required for cell viability in *S. cerevisiae* and *Escherichia coli*. The β-subunits (Sec61β in mammals, Sbh in *S. cerevisiae*, Secβ in archaea) are not essential for cell viability in these organisms; they are similar in eukaryotes and archaea, but show no obvious homology to the corresponding SecG subunits in bacteria. The α-subunit forms the channel pore, and it is the crosslinking partner of polypeptide chains passing through the membrane[5]. Reconstitution experiments have shown that the Sec61/SecY complex is the essential membrane component for protein translocation[6,7].

The channel itself is a passive conduit for polypeptides and must therefore associate with other components that provide a driving force[1]. In co-translational translocation, the major partner is the ribosome. The elongating polypeptide chain moves directly from the ribosome into the associated membrane channel. The energy for translocation comes from GTP hydrolysis during translation. Many (or perhaps all) cells also have post-translational translocation, in which polypeptides are completed in the cytosol and then transported across the membrane. In yeast (and probably in all eukaryotes), the post-translational translocation partners are another membrane protein complex (the tetrameric Sec62/63p complex) and the lumenal protein BiP, a member of the Hsp70 family of ATPases[8,9]. BiP promotes translocation by acting as a molecular ratchet, preventing the polypeptide chain from sliding back into the cytosol[10]. In the eubacterial post-translational pathway, the cytosolic ATPase SecA pushes polypeptides through the channel[11]. In addition, an electrochemical gradient across the membrane stimulates translocation *in vitro* and is essential *in vivo*[12]. Archaea lack SecA and the Sec62/63p complex, and it is unclear how they perform post-translational translocation[13]. Despite the differences between the pathways, most mechanistic aspects of translocation that relate to the channel itself are probably similar. Specifically, in all cases the channel partner—either the ribosome, the Sec62/63p complex or SecA—binds first, and the signal sequence or TM of a translocation substrate associates with the channel subsequently, priming it for polypeptide translocation.

An understanding of the mechanisms that underlie protein translocation requires detailed structural information. Low-resolution structures have been obtained by single-particle electron microscopy (EM) of either the isolated Sec61/SecY complex or the Sec61 complex bound to the ribosome[14–18]. A recent structure of the *E. coli* SecY complex, derived from electron cryo-microscopy of two-dimensional (2D) crystals in a phospholipid bilayer, indicated the expected number of TM helices, but the resolution (about 8 Å in-plane) was insufficient for their identification[19]. We now report the structure of the SecY complex from the archae *M. jannaschii*, determined by X-ray diffraction at 3.2 Å resolution.

Structure determination of the SecY complex

We purified and crystallized the complex from *M. jannaschii* in the detergent diheptanoylphosphatidyl choline. Crystals of selenomethionine-derivatized protein diffract to 3.4 Å and have different unit-cell dimensions, depending on buffer conditions (see Supplementary Table 1). Initial phases were obtained from single-wavelength anomalous dispersion (SAD) experiments and improved by a combination of cross-crystal averaging, solvent

flattening and histogram matching. After obtaining an initial model, we generated point mutants in the α-subunit aimed at strengthening crystal contacts. One double mutant (Lys422Arg and Val423Thr), called Y1, gave crystals that diffracted to 3.2 Å. There are subtle differences between the mutant and wild-type structures (see Supplementary Fig. S2), and we have used the latter to generate the figures below. The final wild-type model includes all residues, with the exception of some at the termini (α-subunit 434–436; β-subunit 1–20, 53; γ-subunit 67–73). Examples of the fit into the experimental electron density map are shown in Supplementary Fig. S3, and a summary of the quality of the structures is given in Table 1.

Architecture of the SecY complex

General characteristics

The crystal structure contains a single copy of the SecY complex with one polypeptide chain of each of the three subunits. Figure 1a shows a stereo view from the cytoplasm ('top view') and Fig. 1b shows the complex from the side (for more details, see Supplementary Fig. S4). As expected (see ref. 4), the α-subunit contains ten TMs with amino and carboxy termini in the cytosol, and the β- and γ-subunits have one TM each, with their N termini in the cytosol. Viewed from the top, the SecY complex has an approximately rectangular shape (Fig. 1a). The α-subunit is open on one side (the 'front') and is surrounded on the remaining three sides by the two smaller subunits. The side view shows that only the cytoplasmic domains protrude significantly beyond the phospholipid-head-group region of the membrane (Fig. 1b).

The α-subunit

This subunit is divided into two halves, TM1–5 and TM6–10 (Fig. 1c), which are connected at the back of the molecule by an external loop between TM5 and TM6. Each half consists of three outer and two inner TMs (Fig. 1d) related by pseudo-symmetry through a two-fold rotation axis in the plane of the membrane (Fig. 1d), and they have similar folds (Supplementary Fig. S5). The second half is essentially an inverted version of the first half, and pairs of helices in the two parts are topologically related (for example, TM2 and TM7). A similar pseudo-symmetry that is not obvious from the primary sequence has also been observed in the structures of several other membrane proteins (for example, refs 20, 21).

Many of the TMs in the α-subunit are not perpendicular to the plane of the membrane (for example, TM2, TM5 and TM7), and some do not span the entire membrane (for example, TM9 and TM10). In addition, several loops have a complex secondary structure, and some are tucked back into the membrane (for example, the loop between TM7 and TM8). The most striking feature of the α-subunit is the segment following TM1 (Fig. 1e). In most organisms, it begins with the sequence PΦXG (Φ is a conserved hydrophobic amino acid). It then continues as a long loop that runs along the external side of the molecule before leading back into the centre of the α-subunit and ending in a short, distorted helix, called TM2a. This helix extends to a point about halfway through the membrane (Fig. 1e). It is not particularly hydrophobic and was predicted to be in the external aqueous phase[22]. TM2a is followed by a segment resembling a β-hairpin loop centred on Gly 68 (Supplementary Fig. S3a). This loop ends in the middle of the membrane at the completely conserved Gly 74 of the sequence GΦXP. A sharp turn leads into TM2b, which extends from the centre of the molecule outwards at a ~30° angle with respect to the plane of the membrane.

The β-subunit

This polypeptide begins with a disordered cytoplasmic segment followed by a loop that crosses over the N terminus of the α-subunit (Fig. 1a). The TM is almost perpendicular to the plane of the membrane and comes close to the C terminus of the γ-subunit at the external side of the membrane (Fig. 1b). The β-subunit makes only limited contact with the α-subunit, which may explain why it is not essential for the function of the complex.

The γ-subunit

This subunit consists of two helices. The N-terminal helix lies on the cytoplasmic surface of the membrane (Fig. 1a, b). In agreement with predictions and crosslinking studies[23,24], this helix is amphipathic with the hydrophobic surface pointing towards the membrane, contacting the C-terminal part of the α-subunit. The helix is followed by a short β-strand that forms a sheet with a segment of the β-hairpin between TM6 and TM7 of the α-subunit (Fig. 1a). The TM of the γ-subunit is a long, curved helix that crosses the membrane at a ~35° angle with respect to the plane of the membrane (Fig. 1b). One side of the helix makes limited contacts with TM1, TM5, TM6 and TM10 of the α-subunit, and thus clamps together the two halves of the α-subunit.

Table 1 **Crystallographic statistics**

Data set	SeMet (X25)*	Y1 mutant (8BM)*
Resolution (Å)	3.5	3.2
Unique reflections	14,439 (1,291)	18,118 (1,439)
I/Iσ	30.9 (2.74)	26.9 (2.24)
Completeness (%)	98.4 (89.6)	93.2 (76.1)
R_{sym}†	0.08 (0.67)	0.05 (0.44)
Phasing to 3.8 Å		
FOM (from SOLVE)	0.29 (0.19)	
Map correlation‡	0.24	
Mean phase difference (°)§	75.1 (77.6)	
R_{cryst}‖	0.254 (0.383)	0.242 (0.414)
R_{free}¶	0.334 (0.463)	0.287 (0.442)
r.m.s. deviation bond length (Å)	0.008	0.008
r.m.s. deviation bond angles (°)	1.3	1.23
Mean *B*-factor	122.4	97.8

*Values in parentheses refer to data in the highest-resolution shell (3.63 Å to 3.50 Å and 3.31 Å to 3.20 Å in the wild-type and mutant data sets, respectively). SeMet, selenomethionine.
†$R_{sym} = \Sigma_{hkl}\Sigma_i|I_i(hkl) - I(hkl)|/\Sigma_{hkl}\Sigma_i|I_i(hkl)|$, where $I(hkl)$ is the average intensity. All reflections were used.
‡The map correlation coefficient is the correlation between a synthetic electron density map calculated on the basis of the final model and the map corresponding to the experimental set of phases, averaged over all grid points.
§Mean phase difference between initial phases from SOLVE and phases calculated from the final refined wild-type model. The phase difference is defined as the average difference between experimental phases and phases calculated from the final refined model.
‖$R_{cryst} = \Sigma_{hkl}||F_{obs}| - k|F_{calc}||/\Sigma_{hkl}|F_{obs}|$
¶R_{free} is the same as R_{cryst} for a selected subset (10%) of the reflections that was not included in prior refinement calculations.

Comparison with the EM structure of the *E. coli* SecY complex

Functional interpretations of the X-ray structure must be based on the large body of experimental work carried out on systems from *E. coli*, mammals and *S. cerevisiae*; no functional data are available for archaeal SecY complexes, but the X-ray structure of the *M. jannaschii* complex is probably representative of all species. The amino-acid sequences of the *M. jannaschii* subunits are quite similar to those in eukaryotes and eubacteria (~50% similarity) (Supplementary Fig. S1). Fitting the X-ray structure into the electron density map of the 2D crystal structure of the *E. coli* SecY complex, determined by EM[19], shows that the TM segments of the SecY complexes from *M. jannaschii* and *E. coli* are arranged in nearly identical ways (Fig. 2a). We can identify all TMs in the *E. coli* α-subunit and observe that many features are conserved, including the position of the unusual segment following TM1 (Fig. 2a). The external loops between TM7 and TM8 and between TM5 and TM6 are shorter in eubacteria, causing small shifts in some helices, but the changes are confined largely to lipid-facing parts of the molecule, which have few conserved residues (Supplementary Fig. S6). The agreement between the X-ray and EM models also shows that the architecture is the same whether in detergent solution or in a phospholipid bilayer. Moreover, as the α-subunit in the 2D crystal is part of a dimer[19] (Fig. 2a, b), oligomerization does not grossly change the conformation of the SecY complex.

The small subunits of the *E. coli* complex in the EM structure can

also be identified from a comparison with the *M. jannaschii* complex. The bacterial β-subunit (SecG) comprises two TMs, the second of which has the same position and orientation as the TM of Secβ of *M. jannaschii*[25] (Fig. 2a), suggesting that they may have analogous functions. The N-terminal TM of the bacterial β-subunit (SecG) has no correspondence in archaea and eukaryotes. The γ-subunit (SecE) of *E. coli* has two non-essential TMs at its N terminus[23], which correspond to the two helices that are far apart from the others in the 2D crystal structure of the *E. coli* protein (Fig. 2a). These helices are in approximately the same location as the N terminus of the *M. jannaschii* γ-subunit in the X-ray structure (Fig. 2b).

Translocation pore and plug

Experiments in different systems have shown that the SecY/Sec61p complex forms oligomers during translocation, but as we will argue later, our structure suggests that a single copy of the SecY/Sec61p complex serves as a functional channel. A large, funnel-like cavity with a diameter of 20–25 Å at the cytoplasmic side of the SecY complex could serve as a channel entrance (Fig. 3a, b). It contains many conserved residues (Supplementary Fig. S6), suggesting that it has an important function. The funnel tapers to a close in the middle of the membrane (Fig. 3b), indicating that the structure corresponds to a closed channel, impermeable to polypeptides or even small molecules.

How might the channel open and how could it recognize signals? A large body of data in the literature allows us to propose specific models for these and other properties. TM2a, which we call the 'plug', blocks the bottom of the funnel about halfway across the membrane, and separates the cytoplasmic side from the external aqueous space (Fig. 3a). We propose that the channel opens for polypeptide translocation by displacement of the plug. Consistent with this hypothesis, a cysteine introduced into the plug at residue 67 of the *E. coli* α-subunit (SecY; corresponding to *M. jannaschii* Thr 61) can form a disulphide bridge *in vivo* with a cysteine introduced at residue 120 of the *E. coli* γ-subunit (SecE; *M. jannaschii* residue 64)[26]. These residues are more than 20 Å apart in the closed state of the channel (Fig. 3a). Disulphide bridge formation results in a dominant-negative phenotype, as would be expected if the channel were locked into a permanently open state. Another combination of cysteines (*E. coli* residue 64 in the α-subunit (SecY) and 124 in the γ-subunit (SecE)) is also lethal, whereas combinations of neighbouring residues are not[26], suggesting that the helical structures of the plug and the γ-subunit are maintained during movement. Given that the TM of the γ-subunit is a continuous helix with one hydrophobic side, we assume that it remains stationary while the plug moves as a rigid body into a cavity on the external side of the channel next to the C terminus of the γ-subunit (Fig. 3b, c). This displacement requires a translation of ~22 Å towards the back of the molecule, as well as a shift of about 12 Å towards the external side of the membrane. The hinges for the motion could be the Gly residues at positions 49 and 68. Although not universally conserved, all species have small residues in this region that could serve this function. Movement of the plug would open the pore (Fig. 3b, c), resulting in an hourglass-shaped channel with aqueous funnels that taper to a constriction in the middle of the membrane (Fig. 3b).

The funnel-like cavities on both sides of the constriction would create an aqueous channel across the membrane (Fig. 4a, b). This feature is consistent with fluorescence life-time measurements[3], which suggest that a translocating polypeptide is in an aqueous environment. The walls of both funnel-like cavities contain hydro-

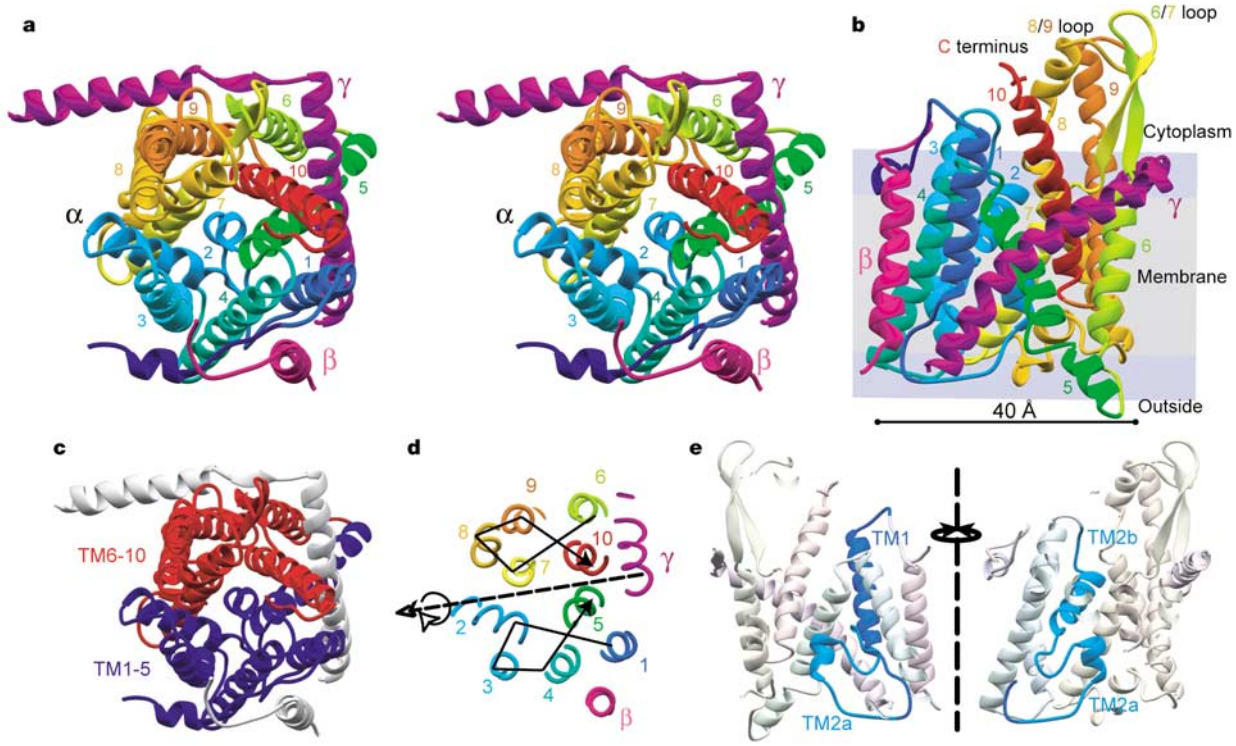

Figure 1 General architecture of the SecY complex. **a**, Stereo view from the cytosol (top). The α-subunit is coloured blue to red from the N to the C terminus with the TM segments numbered; the β-subunit is shown in pink and the γ-subunit in magenta. **b**, View from the back, with the phospholipid head group and hydrocarbon regions of the membrane shown in blue and grey in the background. Cytosolic loops probably involved in ribosome and SecA binding are indicated. **c**, Top view with the N- and C-terminal halves of the α-subunit in blue and red, respectively. **d**, Top view sliced through the middle of the membrane. The solid lines connect the TMs from the N to the C terminus in the two halves; the dotted arrow shows the axis of internal symmetry. **e**, Slab views from the front and back, with the foreground removed and TM1 (dark blue), TM2a and TM2b (sky blue) highlighted.

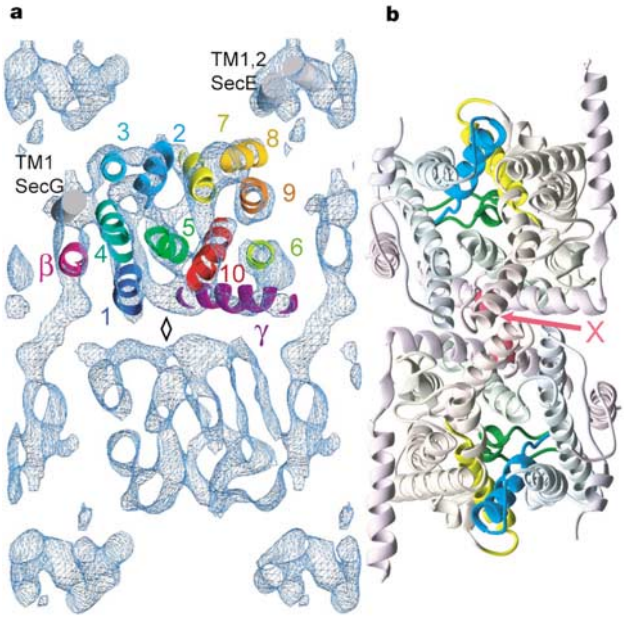

Figure 2 Comparison with the 2D crystal structure of the *E. coli* SecY complex. **a**, X-ray structure of the *M. jannaschii* SecY complex (coloured as in Fig. 1a), visually docked into the electron density map of the *E. coli* SecY complex, determined by cryo-electron microscopy of 2D crystals[19]. Shown is a 5 Å slab, viewed from the top, with the map contoured at 1 σ. The *M. jannaschii* TMs are numbered. TMs of the *E. coli* complex with no correspondence in *M. jannaschii* were fitted into the density as grey cylinders. The diamond symbol indicates the axis of two-fold symmetry in the *E. coli* complex. **b**, Modelled dimer of the SecY complex, in the same orientation as in **a**, with TM2b and TM7 coloured as in Fig. 1a. TM2a (plug) is shown in dark green. A cysteine introduced at the position indicated by a red sphere results in efficient crosslinks (X) between two γ-subunits.

philic residues (Fig. 4a, b), but there are few charges (not shown). The absence of charges is particularly remarkable for the cytoplasmic funnel; its interior is uncharged, but its outer rim in the cytoplasm contains a large number of both positive and negative residues.

The pore ring

The nature of the constriction suggests a mechanism by which the membrane barrier can be maintained during protein translocation. At its narrowest point, the channel is lined by a 'pore ring' of six hydrophobic residues (Ile 75, Val 79, Ile 170, Ile 174, Ile 260 and Leu 406) (Fig. 3b, c). In *E. coli*, the corresponding residues are all isoleucines, and this amino acid is frequently found as pore residues in other species (Supplementary Fig. S1). The opening formed by the ring is about 5–8 Å. The hydrophobic residues may form a gasket-like seal around a translocating polypeptide, and bulky isoleucines may be particularly suitable seal residues. Different amino acids must pass through the pore ring, and the required flexibility may be provided largely by lateral shifts of the helices to which the pore residues are attached (see below). Although the seal is not likely to be perfect, it would significantly hinder the passage of small molecules during translocation. This model is different from previous proposals, in which the ribosome–channel junction and the binding of the lumenal protein BiP provide the seal in co-translational translocation in mammals[3,27]. Our model explains how the membrane barrier can be maintained in both co- and post-translational translocation pathways, and why a gap between the ribosome and the channel, seen in EM structures of the eukaryotic ribosome–channel complex[15–18], may not compromise the membrane barrier.

The hourglass shape of the open channel would minimize its interactions with a translocating polypeptide chain. Contacts would be confined largely to the constriction formed by the pore residues. Because the constriction consists of only a single layer of hydrophobic side chains (Fig. 3b), interactions with a polypeptide at its centre would probably be weak, even when hydrophobic amino acids are passing through. The lack of charges in the cavities on either side of the constriction may also help to minimize interactions between the channel and the translocating chain.

The diameter of the pore ring seen in the X-ray structure might be sufficient to accommodate an extended polypeptide chain, but with a little expansion it could allow passage of an α-helix. An increase in pore size could result from shifts in the helices that line the channel, perhaps facilitated by rearrangement of the loop between TM4 and TM5, in which the conserved Gly residues of a Gly-Ile-Gly-Ser-Gly-Ile-Gly sequence could serve as hinges. TM10 could also move, facilitated by conserved Gly residues in the membrane-embedded loop between TM9 and TM10, related by pseudo-symmetry to the 4/5 loop (Supplementary Fig. S5). These shifts could allow a variable pore width, and might explain how even bulky residues attached to the side chains of amino acids *in vitro*[28] or a disulphide-bonded polypeptide loop of 13 residues in a secretory protein[29] can be transferred through the channel. The pore size would effectively prevent the passage of folded domains, consistent with experimental data[30,31]. Unless the pores of several copies of Sec61p/SecY complexes fuse into a larger pore (see below), the structure seems

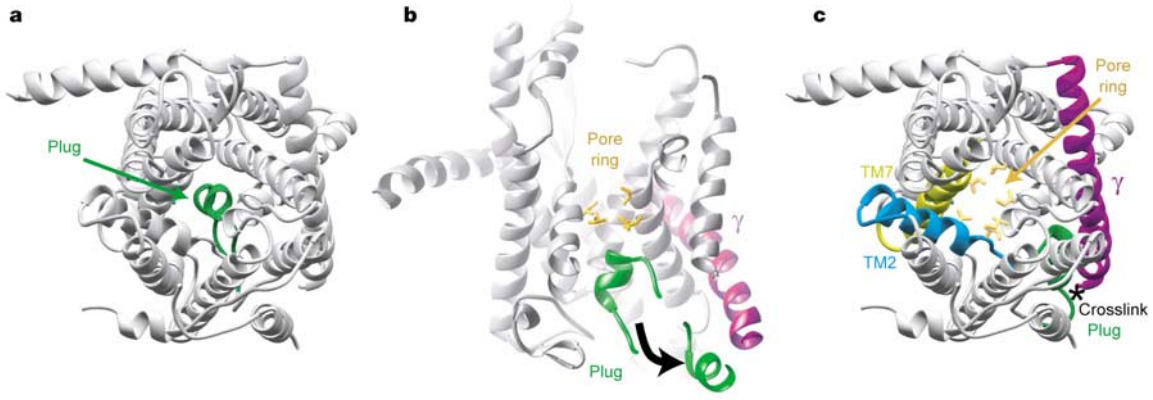

Figure 3 The channel pore. **a**, View from the top with TM2a (plug) coloured in dark green. **b**, View from the side with the front half of the model cut away. The modelled plug movement towards the γ-subunit (magenta) is indicated. The hydrophobic pore ring is shown by the side chains coloured in gold. **c**, Top view with the plug modelled in its open position. TM2b and TM7 are coloured as in Fig. 1a. The star indicates the region where introduced cysteines result in crosslinking between TM2a and the TM of the γ-subunit.

to be inconsistent with the claim that the open channel has a diameter of at least 40 Å (ref. 32).

Signal-sequence binding and lateral gating

One trigger for channel opening is binding of the signal sequence of a translocation substrate[3,33]. At the beginning of translocation of a secretory protein, the polypeptide inserts into the channel as a loop, with the signal sequence intercalated into the walls of the channel and the following, mature region located in the aqueous pore. Photocrosslinking experiments in a yeast *in vitro* system have shown that the hydrophobic region of a bound signal sequence forms a helix of approximately two turns, contacted on opposite sides by TM2 and TM7 (ref. 34). The part of the signal sequence preceding the hydrophobic core contacts TM8 (ref. 34). Each residue of the signal sequence can also be crosslinked to phospholipid molecules, indicating that the binding site is located at the interface between channel and lipid[34]. The X-ray structure of the SecY complex enables us to rationalize these results. The signal-sequence intercalation site is located between TM2b and TM7 at the front of the cytoplasmic funnel (Figs 5a, b); it is not close to the TM of the γ-subunit, as previously proposed[34]. The top of TM2b interacts with TM8, explaining why TM8 can be crosslinked to the N terminus of the bound signal sequence[34]. In addition, the weak crosslinks of the signal sequence to TM2a (designated as TM1 in ref. 34) are also consistent with the structure. The residues forming the signal-sequence-binding site are well conserved (Supplementary Fig. S6). TM2b and TM7 are in opposite halves of the α-subunit, and intercalation of a signal sequence between them would require the front of the α-subunit to open. This could result from a small (~15°) hinge motion between TM5 and TM6 at the back of the molecule (Fig. 5), which would create a pore with dimensions of 15–20 Å front to back and 10–15 Å side to side, sufficient to allow loop insertion of a translocating polypeptide chain. As TM2b and TM7 cross at an angle of about 70°, the signal sequence could not be in contact with both TMs for more than two turns, consistent with the minimal requirement for 6–7 consecutive hydrophobic residues in a functional signal sequence. Small variations in the hinge opening could permit a range of separations and relative orientations of TM2b and TM7, providing the flexibility needed to insert different signal sequences. Intercalation between TM2b and TM7 at the open front of the α-subunit would also explain why the signal sequence is exposed to lipid[34].

The location of the TM2b–TM7 intercalation site is consistent with a role for the signal sequence as a trigger for channel opening[3,33], because the signal sequence would have access to its binding site in the closed channel (Fig. 5b). We propose that the bound signal sequence destabilizes the interactions of the plug that keep it in the centre of the pore, opening the channel. Insertion into the pore of the polypeptide region distal to the signal sequence could fix the channel in the open state by preventing the plug from returning to its closed-state position. The plug could return and the pore would close only after the polypeptide chain had left the channel.

The TMs of nascent membrane proteins must exit laterally from the channel into the lipid phase. The X-ray structure shows that the front is the only place where the complex could open towards lipid; all other directions are blocked by the small subunits or obstructed by segments of the α-subunit. The lateral gate would be formed in the cytoplasmic half of the membrane by the interface between TM2b and TM8 and between TM2b and TM7, and in the external half by the interface between TM3 and TM7 (Fig. 5a, b). Opening the gate would require breaking of hydrophobic interactions and of hydrogen bonds between the conserved Gln 86 in TM2b and Thr 337 in TM8, and between Asn 268 in TM7, Glu 122 in TM3 and Thr 80 in TM2b (the last two are conserved; see Supplementary Fig. S1). Whereas signal sequences contain relatively short hydrophobic segments and may stay intercalated into the lateral gate until they are cleaved by signal peptidase, longer and more hydrophobic TMs may partition into lipid[35].

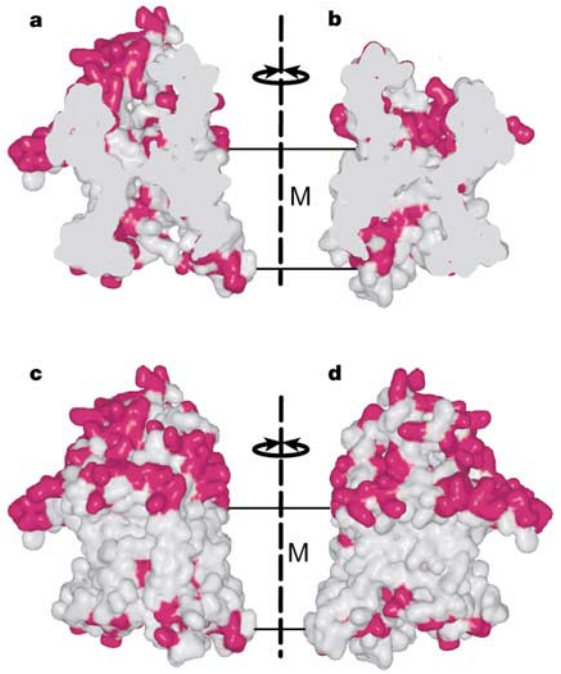

Figure 4 Distribution of polar residues. Accessible surface representations of the channel with the plug in its open-state position and polar amino-acid residues (S,T,C,H,D,E,N,Q,R,K) shown in red. **a**, **b**, Internal surface of the cytoplasmic and external funnels, revealed by cutting the complex into halves. The two views are related by 180° rotation. **c**, **d**, External surface of the complex shown from the front and back. The lines indicate the borders of the hydrophobic region of the membrane (M).

Signal-sequence suppressor mutations

Support for the postulated mechanism of pore opening comes from the location of signal-sequence suppressor (prl) mutations. Genetic studies in *E. coli* have shown that certain mutations in the SecY complex allow secretory proteins with defective or even deleted signal sequences to be transported[36,37]. Most of the prl mutations are located in the centre of the channel, particularly on the internal side of TM7 and in the plug (Fig. 6). Inspection of specific mutations indicates that at least some of them could destabilize the closed state of the channel. For example, the mutations Phe64Cys and Asn65Tyr (prlA300 and prlA8914) in the *E. coli* α-subunit (SecY) correspond to changes in residues within the plug (Phe 58 and Trp 59) that face TM7. Other prl mutations change hydrophobic residues in the pore ring to hydrophilic residues (for example, Ile408Asn (*M. jannaschii* Leu 406) in prlA4). These mutations may stabilize the open state of the channel, in which the residues of the pore are in an aqueous environment, or they may facilitate widening of the pore during initiation of translocation. The prlG3 mutation Ser120Phe in the *E. coli* γ-subunit (SecE; *M. jannaschii* Gly 64) may also stabilize the open state of the channel, as this is the same residue that can be crosslinked to the plug. In general, our analysis supports the idea that prl mutations mimic the effect of signal-sequence binding—that is, they destabilize the closed state of the channel or stabilize the open state.

Binding of cytosolic channel partners

For translocation, the channel must associate with a partner, which can be—depending on the mode of translocation—the ribosome, SecA or the Sec62/63p complex. The ribosome must bind predominantly to the cytosolic domains in the C-terminal half of the α-subunit—that is, to the loops between TM6 and TM7 and between

TM8 and TM9, and to the C-terminal tail (Fig. 1b). Proteolysis experiments with the mammalian Sec61p complex have shown that the loop between TM8 and TM9 and the C-terminal tail are required for high-affinity ribosome binding[38]. The tip of the 8/9 loop contains several conserved residues, including the universally conserved Arg 360 and Arg 372, which are prime candidates for interaction with nucleic acid in the large ribosomal subunit[39]. The cytosolic loops in the N-terminal half are much shorter, hardly protruding beyond the phopholipid-head-group region (Fig. 1b), and would not be expected to make strong contacts. Binding of the ribosome to only one half of the α-subunit would not prevent the relative movement of the two halves, which the structure suggests is required for signal-sequence intercalation. The protrusion of the cytosolic loops in the C-terminal half could place the binding platform for the ribosome 10–20 Å away from the plane of the membrane. A gap of this size has been seen by EM of ribosome–channel complexes[15–18].

In eubacteria, the same cytosolic domains that bind the ribosome probably interact with SecA. The loop between TM8 and TM9 is particularly important, and mutagenesis of residues corresponding to Arg 360 and a few residues following it results in translocation defects (for a review, see ref. 40). Mutations in the C-terminal tail, although not abolishing the interaction with SecA, prevent a conformational change in SecA that is required for translocation[40]. Both the overlap of the interaction sites and size considerations suggest that the ribosome and SecA cannot bind at the same time. The narrow pore in the SecY complex does not explain observations that suggest a deep insertion of SecA into the channel[11,41].

Binding of a channel partner probably causes conformational changes in the Sec61p/SecY complex. This would be consistent with the observation that Sec61p channels with bound ribosomes have an increased conductance for small molecules compared with those without a channel partner or those containing a translocating polypeptide[2,42]. Binding of a channel partner followed by intercalation of a signal sequence may be required to open the channel. In the case of a prl mutant in *E.coli*, SecA binding would be sufficient, and a signal sequence would not be needed.

Oligomerization of the Sec61/SecY complex

The translocating channel is likely to be an oligomer of the Sec61/SecY complex, containing between two and four copies[15–19,43–45], and it has been assumed that a large pore forms at the interface of several Sec61/SecY complexes. However, a side view shows that simple association of several copies of the complex could not form a hydrophilic pore in the membrane (Fig. 4c, d). A hydrophilic pore could be generated by multiple complexes only if they associated at their front surfaces and opened to fuse the α-subunits into a larger channel. The enlarged pore would be lined by the same residues as in a single complex, but would have a lateral exit site at each of the interfaces between α-subunits. Although we cannot exclude this possibility, we consider it unlikely. In fact, for the bacterial post-translational translocation system, experimental evidence suggests that a dimer with a back-to-back association of the complexes is the basic functional unit. This is the arrangement seen in the 2D crystal structure[19] (Fig. 2). A cavity between the two monomers, previously thought to be a potential pore[19], is entirely hydrophobic and is probably filled with lipids. A functional back-to-back association of two SecY complexes is supported by several different experiments. Cysteine crosslinking shows that two γ-subunits are close to one another during translocation[46], with the most efficient crosslinking occurring at residue 106 of the *E. coli* γ-subunit (SecE; *M. jannaschii* Ile 50), which is indeed at the interface between two γ-subunits in the 2D crystals (Fig. 2b). Crosslinking also shows that the N and C termini of two α-subunits are in proximity, and that the crosslinked dimer has translocation activity[47]. A tandem molecule, in which the C terminus of the first α-subunit is linked with the N terminus of the second, is also functional[45]. Because the lateral exit sides in the back-to-back dimer face different directions and there is no connection between the two pores (Fig. 2b), we conclude that one copy of the SecY complex is sufficient to serve as an active pore. In support of this proposal, a detergent-solubilized translocation intermediate contains just one copy of SecY complex associated with one SecA and one translocation substrate molecule[45,48]. The active translocation channel may also be contained in a tetramer of SecY complexes[43], which could

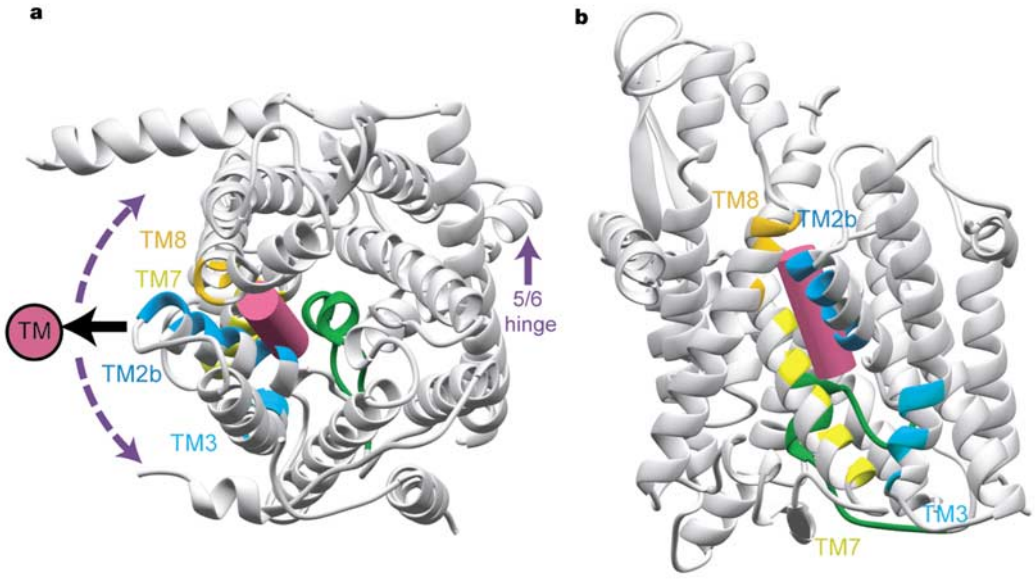

Figure 5 Signal-sequence-binding site and lateral gate. **a**, **b**, Views from the top (**a**) and the front (**b**), with faces of the helices that form the signal-sequence-binding site and the lateral gate through which TMs of nascent membrane proteins exit the channel into lipid highlighted in colours as in Fig. 1a. The plug is coloured in green. The hydrophobic core of the signal sequence probably forms a helix, modelled as a magenta cylinder, which intercalates between TM2b and TM7 above the plug. Intercalation requires opening the front surface, as indicated by the broken arrows, with the hinge for the motion being the loop between TM5 and TM6 at the back of the molecule (5/6 hinge). A solid arrow pointing to the magenta circle in the top view indicates schematically how a TM of a nascent membrane protein would exit the channel into lipid.

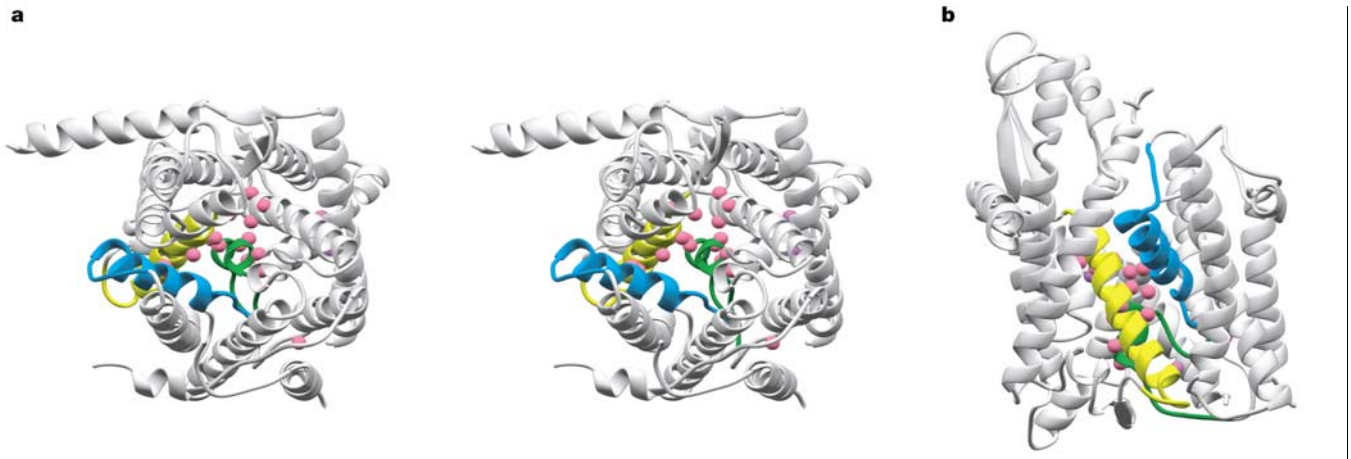

Figure 6 Signal-sequence suppressor (prl) mutations. **a**, Stereo view from the top with the Cβ atoms of the residues corresponding to *E. coli* prl mutations in the α-subunit (SecY) and γ-subunit (SecE) shown as pink and purple spheres, respectively. TM2a, TM2b and TM7 are highlighted in colour. **b**, View from the front.

form by the association of two dimers side by side, similar to their arrangement in the 2D crystal lattice[19]. Crosslinks between the TM of the *E. coli* γ-subunit (SecE) and TM2 and TM7 of the α-subunit (SecY) have been observed[49], but they do not fit with either front-to-front or back-to-back orientation of the monomers.

Ribosome-associated Sec61p channels contain three or four copies of the complex[15–18]. In view of their sequence similarity (Supplementary Fig. S1), it seems likely that the co-translational eukaryotic and the post-translational bacterial complexes function similarly. We therefore favour a model in which two dimers, with a back-to-back arrangement of the complexes, associate side by side beneath the ribosome. The front sides of all complexes would then face outwards, and only one complex at any given time would form the active pore and contain a translocating polypeptide. As the ribosome is asymmetric and would make different contacts with the four copies of the Sec61p/SecY complex, the monomers may have different conformations. Our model implies that the appearance of a pore in low-resolution EM structures of ribosome–channel complexes is simply an indentation between the subunits rather than a channel. The recent higher-resolution EM structures do not have a pore, and the observed central indentation is offset from the exit site of the nascent chain from the ribosome[17,18].

Oligomers of the Sec61p complex may also be required for post-translational translocation in *S. cerevisiae*[14], but there is no evidence that the signal sequence intercalates between TMs of different α-subunits[50]. Thus, in all three translocation pathways, a single copy of the Sec61p/SecY complex in an oligomeric assembly may form the translocation pore.

If the active pore is formed by a monomer, what is the role of oligomerization? Allosteric interactions between the monomers, regulation of the binding of partners and display of sites for recruitment of other factors (for example, signal peptidase, oligosaccharide transferase, TRAM or TRAP) are possible answers. Nonetheless, the issue remains an important puzzle for future work.

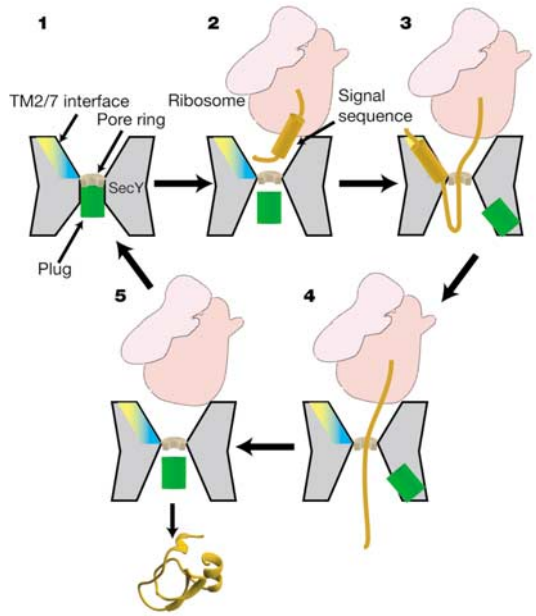

Figure 7 Different stages of translocation of a secretory protein. See main text for description.

A model for protein translocation

The X-ray structure allows us to propose the following refined model for the translocation of secretory proteins. Initially, the channel is closed because the plug blocks the pore (Fig. 7, stage 1). Next, a channel partner binds; depending on the mode of translocation and the organism, this can be a ribosome, the Sec62/63p complex or SecA (Fig. 7, stage 2 indicates the situation with a ribosome). Although part of an oligomer, only one copy of the SecY/Sec61p complex forms the active pore. The closed state of the channel may be destabilized by a conformational change, but binding of the partner alone is insufficient to completely open the channel. In the next step, the substrate inserts as a loop into the channel, with its signal sequence intercalated between TM2b and TM7, and with its mature region in the pore (Fig. 7, stage 3). Insertion requires a hinge motion to separate TM2b and TM7, and displacement of the plug to its open-state position close to the γ-subunit. The mature region of the polypeptide chain is then transported through the pore, and the signal sequence is cleaved at some point during translocation (Fig. 7, stage 4). While the polypeptide chain is moving from an aqueous cytoplasmic cavity to an external one, the pore ring forms a seal around the chain, hindering the permeation of other molecules. Finally, when the polypeptide has passed through, the plug returns to its closed-state position (Fig. 7, stage 5). Membrane protein biosynthesis, although less well understood, might occur in a similar way, except that TMs could move from the lateral gate all the way into lipid, and cytosolic domains would form by emerging through the gap between ribosome and channel. Several of these points differ from conventional

models, but the structure now provides the basis for experimental testing. □

Methods

Protein preparation

We cloned SecY complexes from ten different species into the pBAD22 vector (see Supplementary Information) under control of the arabinose promoter. The plasmids contained the genes for the γ-, α- and β-subunits in this order, each with a separate translation-initiation site. The genes were amplified by polymerase chain reaction (PCR) from genomic DNA, and digested with *Nco*I/*Sal*I, *Sal*I/*Xba*I and *Xba*I/*Kpn*I, respectively. Four-component ligation with *Nco*I/*Kpn*I-digested pBAD22 resulted in the intergenic sequence AGGAGGAGCATC between the 5′ restriction site and the initiation codon of the α- and β-subunits. The γ-subunit contained at its N terminus a hexa-histidine tag followed by a thrombin cleavage site, resulting after cleavage in the N-terminal sequence Gly-Ser instead of Met. The following procedure was used for the SecY complex from *M. jannaschii*, which gave the highest expression levels and was the most stable in a number of detergents. Initially, we crystallized the SecYE dimer, but the crystals never diffracted beyond ~6.5 Å. By consulting sequence databases, we discovered archaeal polypeptides with sequence similarity to the β-subunits in eukaryotes. We co-expressed the β-subunit from *M. jannaschii* and found that it associated with SecYE. The trimeric complex turned out to be significantly more stable than the dimer. For its purification, cells of *E. coli* strain C43 (DE3) were induced with 0.2% arabinose for 3 h at 37 °C or 12–16 h at room temperature, and lysed on ice in TSG buffer (20 mM Tris, 300 mM NaCl, 10% glycerol, pH 7.8) using a microfluidizer. Membranes were collected by centrifugation for 40 min at 40,000 r.p.m., and solubilized in 1.5% (w/v) 1,2-diheptanoyl-*sn*-glycero-3-phosphocholine (DHPC; Avanti Polar Lipids) in TSG buffer. After centrifugation for 30 min at 40,000 r.p.m., the extract was loaded onto a 15–20 ml Ni column (metal-chelating Sepharose, Amersham Pharmacia Biotech). The column was washed with 20 volumes of 0.2% DHPC in TSG buffer in the presence of 30 mM imidazole. The SecY complex was eluted with 300 mM imidazole, exchanged into PBS (pH 7.4) containing 10% glycerol and 0.1% DHPC, and treated with bovine thrombin at 5–10 U mg^{-1} protein for 16 h at 30 °C. After adding imidazole to 30 mM, the solution was passed through a small (2 ml) Ni column. Further purification was carried out by gel filtration on Superdex-200 in buffer A (10 mM HEPES, pH 7.5, 100 mM NaCl, 10% glycerol, 0.1% DHPC), followed by ion-exchange chromatography on Mono-S (Pharmacia) using a gradient from 100 mM to 400 mM NaCl in buffer A. The β-subunit was present at sub-stoichiometric levels relative to the YE subunits; obtaining crystals depended critically on removing contaminating SecYE complexes from the trimeric complex, which was achieved by the gel-filtration and ion-exchange steps. The complex was concentrated to 10–15 mg ml^{-1} with a Centriprep Plus-20 concentrator (Amicon; molecular mass cutoff, 30 kDa) and dialysed overnight at 4 °C.

Selenomethionine-substituted SecY complex from *M. jannaschii* was expressed in wild-type C43 (DE3) cells by inhibition of the methionine biosynthesis pathway. The cells were grown in M9 minimal medium with 0.2% glucose and 5% (v/v) glycerol as carbon sources, and induced with 1% arabinose. Purification was as described for the native protein, with all buffers supplemented with 0.5 mM EDTA and 0.5 mM Tris-(2-carboxyethyl)phosphine to avoid oxidation.

Crystallization

Crystallization of the *M. jannaschii* trimeric SecY complex was performed by hanging-drop vapour diffusion at 4 °C, mixing 1 μl each of protein (5–10 mg ml^{-1}) and reservoir solutions. Initial crystallization conditions were found using a broad screen. After optimization, the best crystals were obtained with 50–55% PEG400, 50 mM glycine buffer, pH 9.0–9.5. They appeared overnight and grew to maximum dimensions of 150 × 150 × 400 μm within a week. They belong to space group $P2_12_12$ and diffract to 3.4 Å. Selenomethionine-substituted crystals of the SecY complex were obtained with ~45% PEG400.

After obtaining an initial model, several double mutants were made in which residues involved in crystal contacts between the C terminus of one monomer and the 5/6 loop of another were changed. One of them (Lys422Arg/Val423Thr), called Y1, crystallized in thin plates at 35% PEG400.

Crystals were flash frozen in liquid nitrogen directly from the drop. We discovered that on gradually increasing the PEG concentration from 35–40% to 52%, the unit cells shrank substantially (Supplementary Table 1). A similar reduction in cell dimensions was observed on soaking certain heavy-atom derivatives such as K_2PtCl_4 into the crystals. The different crystal forms were useful for cross-crystal averaging of electron density maps.

Data collection, structure determination and refinement

Diffraction data were collected at 100 K on beamlines at either the National Synchrotron Light Source at Brookhaven National Labs (X25) or the Advanced Photon Source at Argonne National Labs (8BM, 14BM-C, 19ID) (see Table 1). The data were indexed and scaled with HKL2000. As the crystals were radiation sensitive, we collected highly redundant single-wavelength anomalous dispersion (SAD) data sets at the selenium peak wavelength. Thirteen out of 15 selenium sites were located using SOLVE. The selenium sites in other crystal forms were found by molecular replacement using AMORE. After solvent flattening with CNS, electron density maps were generated with useful phases to ~4 Å. An initial model was built with the program O for the α-helical TM segments, using selenium sites and large amino-acid side chains to determine the registry. The model was improved by an iterative process, using cross-crystal averaging, solvent flattening and histogram matching with a modified version of DMMULTI, and model building. Molecular replacement with the improved model was used in AMORE to obtain electron density maps for the native SecY complex and the Y1 mutant, which were then included in the averaging. Torsion angle refinement with hydrogen bond restraints and B-factor refinement of the model were performed with the Y1 data set using CNS, resulting in an R_{free} of 28.7%. This model was used in the subsequent refinement of the wild-type crystal form, giving an R_{free} of 33.4%. The following residues in the best-refined structure of the α-subunit were poorly defined, presumably because of conformational flexibility: 18–20, 48–55, 288–292 and 301–314. Figures shown in the paper were rendered with RIBBONS and POV-Ray (http://www.povray.org/), except for Fig. 4, which was generated with Raster3D and SPOCK, and Supplementary Fig. S4, which was made using Molscript.

Received 14 October; accepted 19 November 2003; doi:10.1038/nature02218.
Published online 3 December 2003.

1. Matlack, K. E. S., Mothes, W. & Rapoport, T. A. Protein translocation—tunnel vision. *Cell* **92,** 381–390 (1998).
2. Simon, S. M. & Blobel, G. A protein-conducting channel in the endoplasmic reticulum. *Cell* **65,** 371–380 (1991).
3. Crowley, K. S., Liao, S. R., Worrell, V. E., Reinhart, G. D. & Johnson, A. E. Secretory proteins move through the endoplasmic reticulum membrane via an aqueous, gated pore. *Cell* **78,** 461–471 (1994).
4. Rapoport, T. A., Jungnickel, B. & Kutay, U. Protein transport across the eukaryotic endoplasmic reticulum and bacterial inner membranes. *Annu. Rev. Biochem.* **65,** 271–303 (1996).
5. Mothes, W., Prehn, S. & Rapoport, T. A. Systematic probing of the environment of a translocating secretory protein during translocation through the ER membrane. *EMBO J.* **13,** 3937–3982 (1994).
6. Brundage, L., Hendrick, J. P., Schiebel, E., Driessen, A. J. M. & Wickner, W. The purified *E. coli* integral membrane protein SecY/E is sufficient for reconstitution of SecA-dependent precursor protein translocation. *Cell* **62,** 649–657 (1990).
7. Gorlich, D. & Rapoport, T. A. Protein translocation into proteoliposomes reconstituted from purified components of the endoplasmic reticulum membrane. *Cell* **75,** 615–630 (1993).
8. Deshaies, R. J., Sanders, S. L., Feldheim, D. A. & Schekman, R. Assembly of yeast Sec proteins involved in translocation into the endoplasmic reticulum into a membrane-bound multisubunit complex. *Nature* **349,** 806–808 (1991).
9. Panzner, S., Dreier, L., Hartmann, E., Kostka, S. & Rapoport, T. A. Posttranslational protein transport in yeast reconstituted with a purified complex of Sec proteins and Kar2p. *Cell* **81,** 561–570 (1995).
10. Matlack, K. E., Misselwitz, B., Plath, K. & Rapoport, T. A. BiP acts as a molecular ratchet during posttranslational transport of prepro-α-factor across the ER membrane. *Cell* **97,** 553–564 (1999).
11. Economou, A. & Wickner, W. SecA promotes preprotein translocation by undergoing ATP-driven cycles of membrane insertion and deinsertion. *Cell* **78,** 835–843 (1994).
12. Schiebel, E., Driessen, A. J. M., Hartl, F.-U. & Wickner, W. $\Delta\mu H^+$ and ATP function at different steps of the catalytic cycle of preprotein translocase. *Cell* **64,** 927–939 (1991).
13. Irihimovitch, V. & Eichler, J. Post-translational secretion of fusion proteins in the halophilic archaea *Haloferax volcanii*.. *J. Biol. Chem.* **278,** 12881–12887 (2003).
14. Hanein, D. *et al.* Oligomeric rings of the Sec61p complex induced by ligands required for protein translocation. *Cell* **87,** 721–732 (1996).
15. Beckmann, R. *et al.* Alignment of conduits for the nascent polypeptide chain in the ribosome-Sec61 complex. *Science* **19,** 2123–2126 (1997).
16. Menetret, J. *et al.* The structure of ribosome-channel complexes engaged in protein translocation. *Mol. Cell* **6,** 1219–1232 (2000).
17. Beckmann, R. *et al.* Architecture of the protein-conducting channel associated with the translating 80S ribosome. *Cell* **107,** 361–372 (2001).
18. Morgan, D. G., Menetret, J. F., Neuhof, A., Rapoport, T. A. & Akey, C. W. Structure of the mammalian ribosome-channel complex at 17Å resolution. *J. Mol. Biol.* **324,** 871–886 (2002).
19. Breyton, C., Haase, W., Rapoport, T. A., Kuhlbrandt, W. & Collinson, I. Three-dimensional structure of the bacterial protein-translocation complex SecYEG. *Nature* **418,** 662–665 (2002).
20. Murata, K. *et al.* Structural determinants of water permeation through aquaporin-1. *Nature* **407,** 599–605 (2000).
21. Dutzler, R., Campbell, E. B., Cadene, M., Chait, B. T. & MacKinnon, R. X-ray structure of a ClC chloride channel at 3.0 A reveals the molecular basis of anion selectivity. *Nature* **415,** 287–294 (2002).
22. Flower, A. M., Osborne, R. S. & Silhavy, T. J. The allele-specific synthetic lethality of prlA-prlG double mutants predicts interactive domains of SecY and SecE. *EMBO J.* **14,** 884–893 (1995).
23. Murphy, C. K. & Beckwith, J. Residues essential for the function of SecE, a membrane component of the *Escherichia coli* secretion apparatus, are located in a conserved cytoplasmic region. *Proc. Natl Acad. Sci. USA* **91,** 2557–2561 (1994).
24. Satoh, Y., Mori, H. & Ito, K. Nearest neighbor analysis of the SecYEG complex. 2. Identification of a SecY-SecE cytosolic interface. *Biochemistry* **42,** 7442–7447 (2003).
25. Nishiyama, K., Suzuki, T. & Tokuda, H. Inversion of the membrane topology of SecG coupled with SecA-dependent preprotein translocation. *Cell* **85,** 71–81 (1996).
26. Harris, C. R. & Silhavy, T. J. Mapping an interface of SecY (PrlA) and SecE (PrlG) by using synthetic phenotypes and *in vivo* cross-linking. *J. Bacteriol.* **181,** 3438–3444 (1999).
27. Hamman, B. D., Hendershot, L. M. & Johnson, A. E. BiP maintains the permeability barrier of the ER membrane by sealing the lumenal end of the translocon pore before and early in translocation. *Cell* **92,** 747–758 (1998).
28. Kurzchalia, T. V. *et al.* tRNA-mediated labelling of proteins with biotin. A nonradioactive method for the detection of cell-free translation products. *Eur. J. Biochem.* **172,** 663–668 (1988).
29. Tani, K., Tokuda, H. & Mizushima, S. Translocation of proOmpA possessing an intramolecular disulfide bridge into membrane vesicles of *Escherichia coli*. Effect of membrane energization. *J. Biol. Chem.* **265,** 17341–17347 (1990).
30. Mingarro, I., Nilsson, I., Whitley, P. & von Heijne, G. Different conformations of nascent polypeptides during translocation across the ER membrane. *BMC Cell Biol.* **1,** 3 (2000).
31. Kowarik, M., Kung, S., Martoglio, B. & Helenius, A. Protein folding during cotranslational translocation in the endoplasmic reticulum. *Mol. Cell* **10,** 769–778 (2002).
32. Hamman, B. D., Chen, J. C., Johnson, E. E. & Johnson, A. E. The aqueous pore through the translocon has a diameter of 40–60Å during cotranslational protein translocation at the ER membrane. *Cell* **89,** 535–544 (1997).
33. Jungnickel, B. & Rapoport, T. A. A posttargeting signal sequence recognition event in the endoplasmic reticulum membrane. *Cell* **82,** 261–270 (1995).

34. Plath, K., Mothes, W., Wilkinson, B. M., Stirling, C. J. & Rapoport, T. A. Signal sequence recognition in posttranslational protein transport across the yeast ER membrane. *Cell* **94,** 795–807 (1998).
35. Heinrich, S. U., Mothes, W., Brunner, J. & Rapoport, T. A. The Sec61p complex mediates the integration of a membrane protein by allowing lipid partitioning of the transmembrane domain. *Cell* **102,** 233–244 (2000).
36. Bieker, K. L., Phillips, G. J. & Silhavy, T. J. The sec and prl genes of *Escherichia coli.*. *J. Bioenerg. Biomembr.* **22,** 291–310 (1990).
37. Derman, A. I., Puziss, J. W., Bassford, P. J. & Beckwith, J. A signal sequence is not required for protein export in prlA mutants of *Escherichia coli. EMBO J.* **12,** 879–888 (1993).
38. Raden, D., Song, W. & Gilmore, R. Role of the cytoplasmic segments of Sec61α in the ribosome-binding and translocation-promoting activities of the Sec61 complex. *J. Cell Biol.* **150,** 53–64 (2000).
39. Prinz, A., Behrens, C., Rapoport, T. A., Hartmann, E. & Kalies, K. U. Evolutionarily conserved binding of ribosomes to the translocation channel via the large ribosomal RNA. *EMBO J.* **19,** 1900–1906 (2000).
40. Mori, H. & Ito, K. The Sec protein-translocation pathway. *Trends Microbiol.* **9,** 494–500 (2001).
41. Kim, Y. J., Rajapandi, T. & Oliver, D. SecA protein is exposed to the periplasmic surface of the *E.coli* inner membrane in its active state. *Cell* **78,** 845–853 (1994).
42. Heritage, D. & Wonderlin, W. F. Translocon pores in the endoplasmic reticulum are permeable to a neutral, polar molecule. *J. Biol. Chem.* **276,** 22655–22662 (2001).
43. Manting, E. H., van Der Does, C., Remigy, H., Engel, A. & Driessen, A. J. SecYEG assembles into a tetramer to form the active protein translocation channel. *EMBO J.* **19,** 852–861 (2000).
44. Mori, H. *et al.* Fluorescence resonance energy transfer analysis of protein translocase. SecYE from *Thermus thermophilus* HB8 forms a constitutive oligomer in membranes. *J. Biol. Chem.* **278,** 14257–14264 (2003).
45. Duong, F. Binding, activation and dissociation of the dimeric SecA ATPase at the dimeric SecYEG translocase. *EMBO J.* **22,** 4375–4384 (2003).
46. Kaufmann, A., Manting, E. H., Veenendaal, A. K., Driessen, A. J. & van der Does, C. Cysteine-directed cross-linking demonstrates that helix 3 of SecE is close to helix 2 of SecY and helix 3 of a neighboring SecE. *Biochemistry* **38,** 9115–9125 (1999).
47. van der Sluis, E. O., Nouwen, N. & Driessen, A. J. SecY–SecY and SecY–SecG contacts revealed by site-specific crosslinking. *FEBS Lett.* **527,** 159–165 (2002).
48. Yahr, T. L. & Wickner, W. T. Evaluating the oligomeric state of SecYEG in preprotein translocase. *EMBO J.* **19,** 4393–4401 (2000).
49. Veenendaal, A. K., van der Does, C. & Driessen, A. J. Mapping the sites of interaction between SecY and SecE by cysteine scanning mutagenesis. *J. Biol. Chem.* **276,** 32559–32566 (2001).
50. Plath, K., Wilkinson, B. M., Stirling, C. J. & Rapoport, T. A. Interactions between Sec-complex and prepro-α-factor during posttranslational protein transport into the ER. *Mol. Biol. Cell* (in the press).

Supplementary Information accompanies the paper on **www.nature.com/nature**.

Acknowledgements We thank R. MacKinnon for advice and suggestions of reagents; F. Duong for clones; J. Walker for C43 cells; C. Vonrhein, T. Terwilliger and K. Cowtan for help with software; M. Becker, L. Berman and S. LaMarra for support at beamline X25 at the National Synchrotron Light Source (Brookhaven National Laboratory, supported by the US Department of Energy, Division of Materials Sciences and Division of Chemical Sciences); A. Joachimiak, S. Ginell and R. Alkire for help at beamline 19ID at the Advanced Photon Source (supported by the US Department of Energy, Office of Science, Office of Basic Energy Sciences); and C. Ogata and M. Capel for help at beamline 8BM at the Advanced Photon Source (Northeastern Collaborative Access Team supported by an award from the National Center for Research Resources at the National Institutes of Health). We thank C. Akey, V. Ramakrishnan and particularly K. Matlack for critical reading of the manuscript. This work was supported by a fellowship from the Damon Runyon Cancer Research Foundation to W.M.C., and by fellowships from the Human Frontier Science Program Organization to I.C. and Y.M. E.H. was supported by grants from the Deutsche Forschungsgemeinschaft and Fonds der Chemischen Industrie. T.A.R and S.C.H. are Howard Hughes Medical Institute Investigators.

Competing interests statement The authors declare that they have no competing financial interests.

Correspondence and requests for materials should be addressed to T.A.R. (tom_rapoport@hms.harvard.edu). Coordinates for the native and mutant SecY complexes have been deposited in the Protein Data Bank, accession codes 1RHZ and 1RH5, respectively.